

Stability analysis of linked AC power networks with multiple terminal DC grids

Prakash Kumar Sahoo

College of Engineering Bhubaneswar, Odisha, India

Keywords: HVDC, Offshore Grids, Multi-terminal HVDC, Small-signal Stability, System Interactions.

Abstract

This paper presents selected case studies of small-signal stability analysis for power systems consisting of interconnected AC and DC sub-systems. The analysis is based on the Cigré DC-grid test system, which is designed to resemble a generalized future configuration of multi-terminal HVDC (MTDC) systems. The small-signal stability of the system is investigated to identify critical modes associated with different parts of the interconnected AC and DC power systems. The analysis is presented in several steps in order to identify interaction problems and critical modes that can occur with different typical system configurations. Firstly, a case with point-to-point HVDC connection is analysed, followed by the analysis of a four-terminal DC system, before the stability of the entire Cigré DC grid configuration is studied. The state variables participating in critical modes, and the parameter sensitivities of these modes are identified and discussed. The obtained results illustrate particular challenges that can occur during a step-wise construction of a large-scale MTDC transmission system.

1 Introduction

With the expected developments of large scale offshore wind farms at long distances from shore, HVDC transmission based on Voltage Source Converters (VSCs) is emerging as the preferred solution for interconnection with the existing onshore power systems [1]-[3]. In the long term, it is also expected that HVDC transmission systems for wind farms are going to be interconnected with VSC-based point-to-point HVDC interconnections between existing AC grids and gradually form MTDC grids. Such plans are especially relevant in the North Sea region, due to the significant plans for offshore activities related to renewables and oil exploration requiring infrastructure for electric power transmission, as well as the possible benefits of more interconnections among the countries surrounding the North Sea [3], [4]. Similar plans for offshore MTDC grids are also considered in the Mediterranean region [5], and for the east coast of the US [6]. Meshed VSC-based HVDC grids have further been envisioned as a large scale overlay grid to avoid power system limitations and congestions in mainland Europe [3]. Although there are still significant challenges with the

implementation of protection systems and interruption of fault currents in HVDC grids, construction and operation of large-scale MTDC systems is considered technically feasible with available cables and VSC technology. A large range of studies on modelling, control and operation of VSC-based MTDC system have therefore been published in the last few years [7]-[12]. They include examples of stability analysis for hybrid networks comprising AC and DC subsystems [13], accounting for the dynamic effect of synchronous generators in the AC grids [9], [11]. However, since there are not yet any practical installations or established test systems available for large-scale MTDC grids, previous studies have been based on simulations of various system configurations and parameters depending on the main issue under investigation. Thus, the B4 working groups of Cigré have recently proposed a DC grid test system intended as a common reference allowing for easier comparison of results from various types of investigations [14].

This paper will present and discuss the results of small-signal stability analysis of HVDC transmission systems based on the Cigré DC grid test system from [14]. The analysis aims at identifying critical modes of the interconnected AC and DC power systems and revealing how these modes are associated with the grid configuration and the various parts of the HVDC converter controllers. The results from studies of point-to-point HVDC connections constituting sub-systems of the full Cigré DC grid will be presented as a starting point. The study of the basic point-to-point configurations is followed by the analysis of a four-terminal sub-system, before proceeding to the analysis of the full Cigré DC grid test system. Based on the results from these cases, the paper will attempt to identify the oscillation modes that can occur when multiple HVDC converters are connected into a meshed MTDC grid similar to the envisioned development of the North Sea HVDC grid.

2 Investigated System Configurations

The DC grid test system proposed by the Cigré B4.57 working group in [14] and its associated parameters are the starting point for the following investigations. An overview of this system is shown in Fig. 1, indicating the AC and DC grid configurations as well as all converters included in the modelling. Dashed lines in this figure represent cables, while solid lines represent overhead lines. The lengths in km are indicated for each section of the transmission systems. The system contains two onshore AC systems, four independent

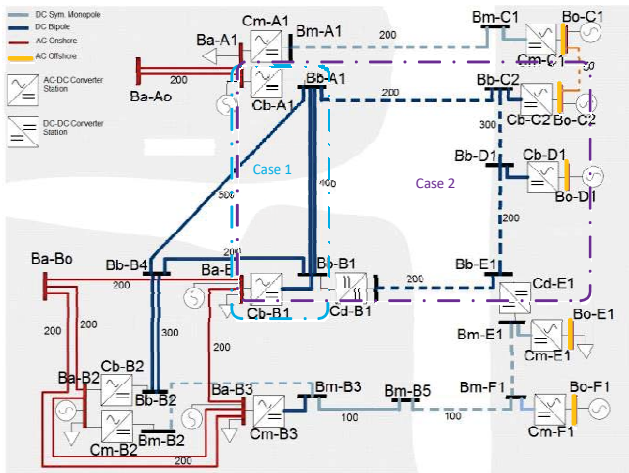


Fig. 1. CIGRE DC Grid Test System [14]

Bus	Bus Type	Generation [MW]	Load [MW]	system
Ba-A0	Slack	S=10 GVA, R/X=0.1		Onshore
Ba-B0	Bus	$\lambda=5$ MW/mHz, T=10 s		Onshore
Ba-A1	PQ	-2000	1000	Onshore
Ba-B1	PQ	-1000	2200	Onshore
Ba-B2	PQ	-1000	2300	Onshore
Ba-B3	PQ	-1000	1900	Onshore
Ba-C1	PQ	-500	0	Offshore
Ba-C2	PQ	-500	0	Offshore
Ba-D1	PQ	-1000	0	Offshore
Ba-E1	PQ	0	100	Offshore
Ba-F1	PQ	-500	0	Offshore

Table 1: Data for the AC bused used in this work

offshore AC systems, and three DC systems. The data for the AC busses is given in Table 1. The two meshed DC grids shown in the lowest part of the figure are interconnected through a DC-DC converter. The system voltages are 380 kV and 145 kV RMS line-to-line for the onshore and offshore AC systems, respectively and 400 kV DC for each AC-DC converter. Thus, the symmetric monopole DC connections have rated voltages of ± 200 kV, while the bi-pole connections are rated for ± 400 kV.

The VSC converters are modelled by average models represented by a current source on the DC-side and a three-phase voltage source on the AC side. The overall control structure of the VSC for different control objective and droop implementation is shown in Fig. 2 and Fig. 3, respectively. The DC-DC converters are modelled according to the same approach with a current source on the high voltage side and a voltage source on the lower voltage side. Since the converters are considered as ideal, all losses are represented by external passive elements. The main physical parameters required for modelling the system are available from [14].

3 Simulation Results and System Analysis

All cases have been modelled and simulated in the DIgSILENT PowerFactory environment. This software has two simulation options; one based on simplified electrical transient phasor models (RMS) and the other based on

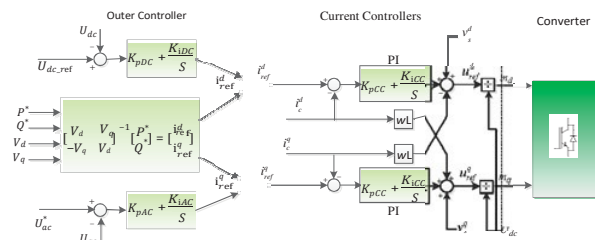


Fig. 2. Overall Control Structure of VSC

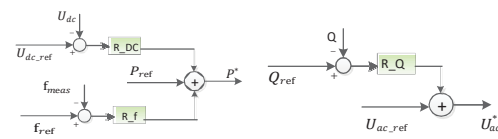


Fig. 3. Droop Control Implementation

Electromagnetic Transient models (EMT). Electromagnetic dynamics of electrical networks are neglected in the RMS simulation, and AC voltages and currents are represented only by their magnitude and phase angle. In EMT simulation voltages and currents are represented by their instantaneous values where dynamic behavior of the network components is also included. For transient stability analysis as well as evaluation of designed control system in large-scale systems, the RMS simulation mode is more suitable since it requires less computation time and enables small-signal analysis of a linearized system model.

Stability analysis of point-to-point HVDC connections

The investigated point-to-point bi-pole VSC-HVDC transmission system is shown in Fig. 4. In this case the bi-pole converter Cb-A1 controls the AC and DC voltages, whereas Cb-B1 controls real and reactive powers. Each converter unit is rated 1200 MVA, has 75 μ F DC link capacitance and is connected to the AC grids through a 380/204 kV two winding transformer with the same MVA rating as the converter. The converter stations are connected through ± 400 kV DC overhead lines (OHL), so the total DC link voltage rating of one bi-pole converter station is 800 kV with a total power rating of 2400 MVA

The small signal stability of this system is investigated for different values of the short circuit ratio (SCR) of the grid. This investigation confirms how the system becomes unstable if the grid becomes weak [15], [16]. In this case the system is unstable if $SCR < 2$ and the power transfer is high (> 0.5 pu) and in case of SCR reduced to 1, the system can only transfer about 50 % of rated power, without provoking a voltage collapse. The trajectory of the eigenvalues for different SCR with 0.625 pu power reference is shown in Fig. 6, where the SCR is varied from 4 to 1. These modes are calculated in PowerFactory by selective modal analysis using the Arnoldi/Lanczos method. A pair of complex conjugate poles corresponding to the PLL of converter Cb-A1 shown in Fig. 6 is responsible for the instability and is moving towards unstable region if SCR is lower than 1.75. Another complex conjugate poles with relatively slow response-, associated

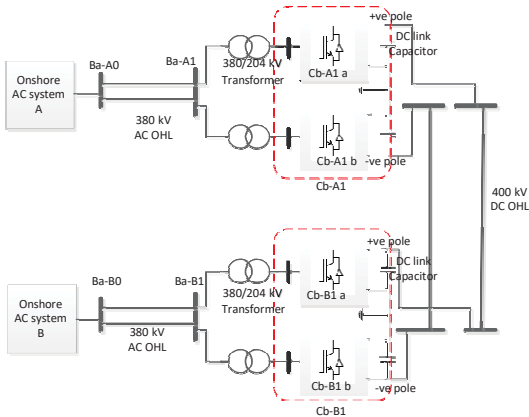


Fig. 4. Investigated bi-pole point-to-point HVDC system (case 1 as indicated with a light blue dash-dotted line in Fig. 1)

with PLL of converter Cb-B1 is also moving towards the real axis. Moreover, some other poles are found to be influenced, for example two complex conjugates poles related to dc voltage measurement filter and dc capacitor of converter station Cb-A1 are moving towards the imaginary axis, but they have less impact of the system dynamics in this case.

Considering the electrical parameters in [14], and properly tuned parameters for the controllers in the system, the investigated case is stable. However, the system can easily become unstable for disadvantageous combinations of controller parameters. The system is therefore first studied without AC transmission lines, and operates properly for current controller proportional gain of 0.5 and integrator time constant of 0.01 s. The proportional gain of the DC-link voltage controller is 2 and the integrator time constant is 0.1 s. However, including the two AC transmission lines in the system (Fig. 4), two pairs of unstable complex conjugate eigenvalues at $17.005 \pm j86.755$ and $1.684 \pm j21.472$ are found for full loading. These modes are mainly influenced by the frequency and voltage angle of AC system, the PLLs and the integrator of the DC voltage controller. This instability effect is the same as for the low SCR, and is confirmed with EMT and RMS simulations. The resulting AC voltage of the converters with this tuning for a step from 0.75 pu to 0.85 pu power reference is presented in Fig. 5. This figure clearly shows how the voltage becomes unstable and quickly collapses at the rectifier terminal, bringing the entire system into instability. It should also be noticed that the analysis confirms how the system can become unstable due to the tuning of the PI controller of the PLLs [15].

For further investigations, the system is made stable by increasing the current controller gain to 4. Then, the following operating condition is specified: AC voltage reference of 1.0 pu and DC voltage reference of 1.01 pu for converter station Cb-A1, active power reference of 0.625 pu and reactive power reference of 0.0 pu for converter station Cb-B1. The corresponding system eigenvalues found from small signal analysis are shown in Fig. 7 (a). They are sorted manually according to their dominant participation factors, and plotted with different colors and markers to identify the

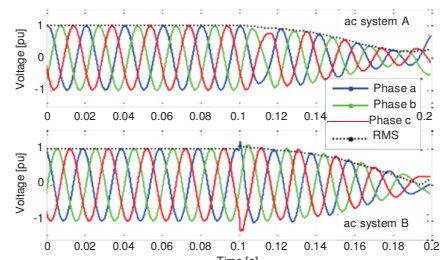


Fig. 5. The AC voltages of the bipole point-to-point HVDC system with weak grid of SCR 2 for stepping power from 0.75 pu to 0.85 pu at 0.1 s

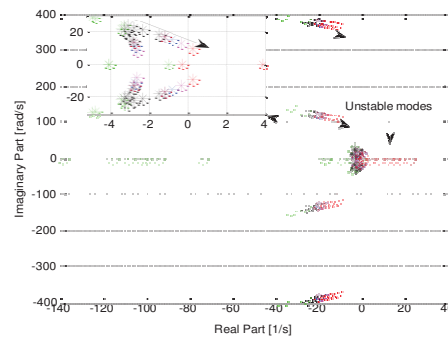


Fig. 6. Eigenvalue trajectory for bi-pole point-to-point HVDC system with SCR of 1-4 of the ac grid

various types of poles. As the system has satisfactory performance, there are no unstable modes, but there are eight pairs of oscillating modes that can be noticed in Fig. 7 (a). The most oscillatory of these pole pairs are located at $-37.226 \pm j397.812$ and $-26.558 \pm j387.017$, corresponding to a damped oscillation frequency of 63.04 and 61.45 Hz, and are found to be mainly associated with the DC link capacitance and DC transmission line of the system. There are also four pole pair with relatively slow damping at $-4.918 \pm j29.413$, $-4.744 \pm j28.751$, $-3.301 \pm j24.457$ and $-3.440 \pm j22.127$ associated with the integrator of the PLL. The last two pair of complex conjugate poles is located at $-26.548 \pm j 132.55$ and $-4.918 \pm j29.413$, and has a relatively fast response related to the use of measurement filters in the converter control.

A symmetrical monopole point-to-point VSC HVDC system with the same rating and control condition as the studied bi-pole configuration has also been investigated for comparison. In this case the rating of the transformers is increased to 2400 MVA and the converter side voltage is 408 kV. To be equivalent to the bi-pole converter station, the DC voltage of the symmetric monopole converter is 800 kV and the DC link capacitance is 37.5 μ F. The resulting eigenvalues of this system under the same operating conditions as the bi-pole connection are shown in Fig. 7 (b). Comparing the eigenvalues for the bi-pole and monopole configurations it is clearly seen that the bi-pole has twice the number of poles, and that the most noticeable poles are doubled poles in similar locations as the corresponding eigenvalues for the monopole system. It is especially noticeable how the most oscillatory poles have higher oscillation frequency, but also a more negative real part for the bi-pole configuration than the

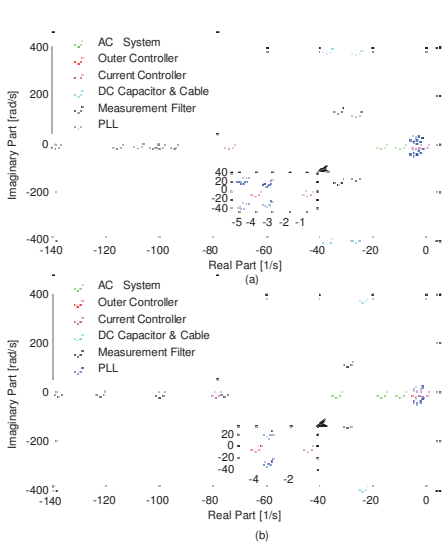


Fig. 7. Eigenvalue plot of (a) point-to-point bi-pole VSC HVDC system and (b) monopole equivalent to the investigated bi-pole point-to-point HVDC system

equivalent monopole configuration. From a general comparison of the bi-pole configuration and the equivalent monopole configuration it is also noticed that some of the real poles have quite different locations. However these are all fast poles with no critical influence on the operation of the system. The poles close to 0 are all the same for both systems, except that the bi-pole configuration has double sets of poles located very close to each other.

Stability analysis of four terminal HVDC System

In this case, two more bi-pole VSC converters, Cb-C2 and Cb-D1 are added to the system from case 1. Both converters are operated as AC slack converters, connecting two independent offshore wind farms to the DC system. The power rating of Cb-C2 is 2x400 MVA and Cb-D1 is rated for 2x800 MVA. As for the other offshore systems, the AC voltage is 145 kV, and the 204/145 kV transformers have the same ratings as the corresponding converters. Each of the wind farms is producing 500 MW, and the resulting power flow of the system is indicated in Fig. 8. The power produced by the wind farms is exported to the onshore system B through the DC grid, together with some additional power injected from the onshore system A.

The small signal stability of the system is analyzed and it is found that the system is oscillatory unstable with the 75 μF DC capacitances of converter station Cb-B1 used for the bi-pole point-to-point system in case 1. Since this mode is sensitive to the DC link capacitance, this value is increased to 312 μF, ensuring that the system has sufficient stability margin at full loading. The resulting eigenvalues of the stable four terminal system are plotted in Fig. 9. It can be seen from this figure, that the system has always double sets of complex conjugate poles, since it is a bi-pole configuration, and that most of these poles are located in similar positions as for the point-to-point connection. Since the added converters are

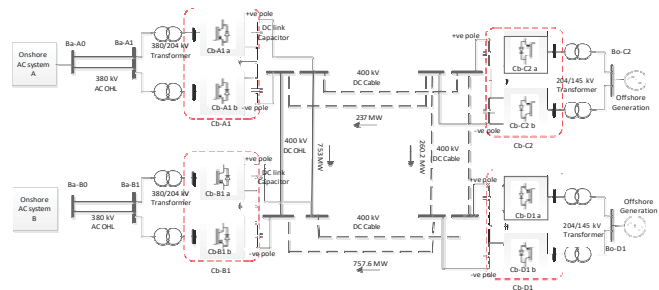


Fig. 8. Schematic of investigated Four Terminal HVDC system (Case 2 as indicated with purple dash-dotted line in Fig. 1)

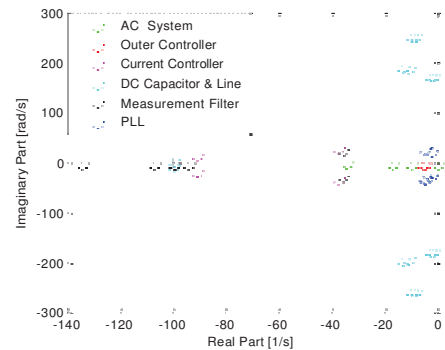


Fig. 9. Eigenvalue plot of four terminal HVDC system

operated as slack busses without much dynamics of the control, there are not significant new poles with high oscillation frequencies related to the DC capacitances introduced in the system. There is however an additional set of double pole pairs associated with the measurement filters of the converters. There are also additional sets of complex poles close to the real axis, whereof one of them have relatively poor damping. Time domain simulations have also been carried out to further investigate how the poles of the system influence the dynamic response of some of the main variables. One example of such simulations is shown in Fig. 10, showing the dynamic response of the AC voltages at selected busses in the system when there is a change in wind power injection into the DC grid. Starting from steady-state, the output power of the wind farm connected to bus Bo-C2 is increased by 20 % at 0.5 s of simulation time, and at 1.3 s the output power of the wind farm connected to bus Bo-D1 is decreased by 20 %.

Further studying the results in Fig. 9 and Fig. 10 it can be found that the oscillation mode at $-37.60 \pm j28.41$ is corresponding with the voltage oscillation of bus Ba-A1. This oscillation mode is associated with measurement filter of DC voltage, the PI controller of the PLL and the DC voltage controller. Similarly, voltage oscillation at bus Ba-B1 is coinciding with the oscillation mode given by the complex pole at $-2.37 \pm j23.385$. The real part of this eigenvalue is small, and it therefore takes a relatively long time to damp the oscillation. The state of the PLL for the converter Cb-b1 has a high participation factor in this mode. The voltage oscillations at busses Bo-C2 and Bo-D1 are mainly corresponding to the eigenvalues at $-1.41 \pm j174.75$ and $-12.91 \pm j191.77$, respectively. The PLL of the corresponding converter has a

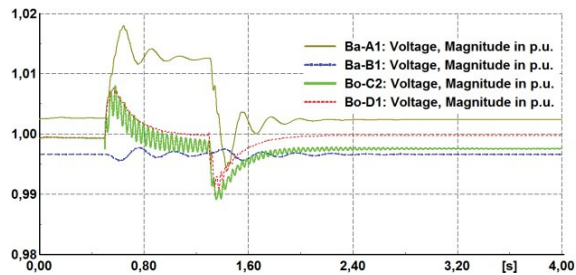


Fig. 10. AC voltage of four terminal HVDC system with two transient events at 0.5 s and 1.3 s

high participation in the oscillation at bus Bo-D1. The oscillation at bus Bo-C2 is however much more poorly damped, and is closely associated to the measurement filters. It is noticeable from Fig. 7 and Fig. 9 that in the four terminal system the most oscillatory poles associated with DC link capacitor and line are now closer to the imaginary axis. The fast poles corresponding to the current controller also become oscillatory in this case, although they are well damped.

Stability analysis of the Cigré DC Grid Test System

To study the dynamics of a more complex system, the full Cigré DC grid test system is investigated. An overview of all the AC-DC converters and their control modes and reference set-points is given in Table 2. The current controller proportional gain is in the range 2-0.4 depending on the parameters and rating of the converter and integrator time constant is kept 0.01 s. The DC and AC voltage controller proportional gain and integral time constant are 2, 0.1 s and 6, 0.25 s, respectively. As can be seen in this table, AC frequency droop and DC voltage droop are included in the control systems of the converters controlling active power. Similarly, the converters used to control AC voltages are applying a reactive power droop. The droop gains have significant impact on stability of the systems and must therefore be carefully selected. A simulation of the voltages in the onshore and offshore systems is presented in Fig. 11. It can be seen that the AC system voltage at bus Ba-A1 is close to 1 pu since the converter connected to that bus is controlling the AC voltage. The voltage at bus Ba-B1 is however higher because the converter at that bus is injecting real power to the AC system while controlling 0 reactive power. The AC system voltages of all the onshore busses are also within their operating ranges from 0.95 pu to 1.05 pu. In the offshore wind farm systems C, the voltages are slightly above the nominal values since the AC cables are producing reactive power. Converter Cb-C2 is exporting power to the DC system and producing reactive power. Proper AC voltage control is obtained by implementing a reactive power droop at that converter. The resulting voltage has a slightly oscillatory response during transient events but the system is stable and steady state operation is satisfactory.

Small signal stability of the system is studied for various control conditions. Without reactive power droop at converter Cb-C2 the AC voltage controller trying to control the bus voltage provokes instability, with a real positive pole in

AC-DC Converter	Control Objective and set-point	
	Active Power	Reactive Power
Cm-A1	$V_{DC,ref} = 1\text{pu}$	$Q_{ref} = 0$
Cm-C1	AC Slack	
Cm-B2	$V_{DC,ref} = 0.99\text{pu}$	$Q_{ref} = 0$
Cm-B3	$P_{ref} = 0.75\text{ pu}$ Droop on V_{DC} and f_{AC}	$V_{AC,ref} = 1\text{pu}$ Droop on Q
Cm-E1	AC Slack	
Cm-F1	AC Slack	
Cb-A1	$V_{DC,ref} = 1.01\text{pu}$	$V_{AC,ref} = 1\text{pu}$ Droop on Q
Cb-B1	$P_{ref} = 0.625\text{ pu}$ Droop on V_{DC} and f_{AC}	$Q_{ref} = 0$
Cb-B2	$P_{ref} = 0.71\text{ pu}$ Droop on V_{DC} and f_{AC}	$Q_{ref} = 0$
Cb-C2	$P_{ref} = -0.75\text{ pu}$ Droop on V_{DC} and f_{AC}	$V_{AC,ref} = 1\text{pu}$ Droop on Q
Cb-D1	AC Slack	

Table 2: Overview of Converters and Control Objectives

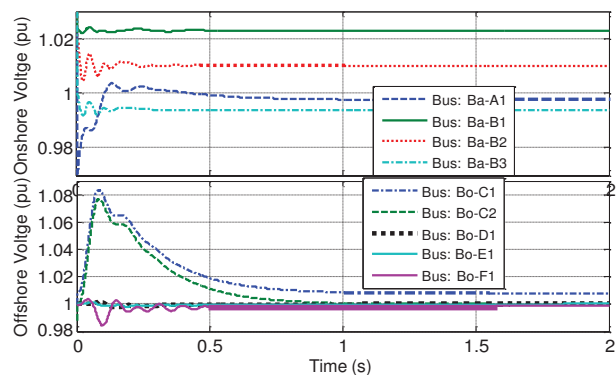


Fig. 11. Offshore and onshore voltage of CIGRE DC Grid Test system for stable operation

33.728. Stability is also studied without reactive power droop at converter Cm-B3 resulting in an unstable eigenvalue at 9.337. In this case, the AC voltage controller state has high participation in the unstable mode, but the AC voltage measurement filter and the PLL of Cb-B1 are also contributing. There is an unstable mode at $1.974 \pm j31.199$ without AC voltage droop for converter Cb-B1, where the corresponding PLL has high participation factor. However, the PLL of Cb-B2, the integrator of the DC voltage controller of converter Cb-A1, the frequency of the AC system A and the measurement filters are also associated with this mode.

Considering the full Cigré DC grid test system in stable operation, a selected plot of the most important eigenvalues is shown in Fig. 12. From this figure, the most oscillatory poles that occur when expanding the system appear to be related to the DC-link capacitors of the converters. The poles associated with the current controller show similar behavior as four terminal system when it expands point-to-point to multi terminal system. There are also a significant set of complex conjugate poles with low oscillation frequencies related to the PLLs and the outer controllers of the converters, and some additional oscillatory poles with more negative real values associated with the measurement filters of the control systems. However, the grouping of the poles is not changing

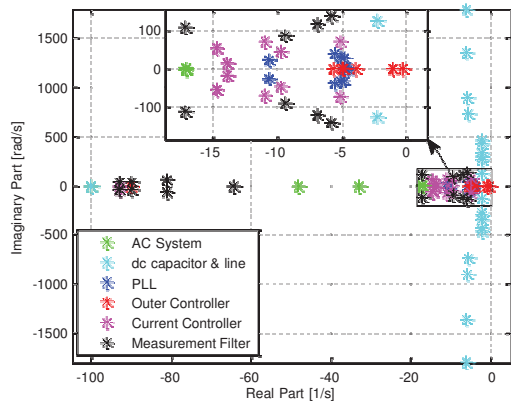


Fig. 12. Selective Eigenvalue plot of Cigré DC Grid Test system for stable operation with SCR 4

significantly by expanding the system, as long as individual converters are kept in stable operation. Although further, and more systematic, analysis is required, this indicates that such MTDC system can easily be expanded step by step, as long as sufficient care is taken on the design and tuning of the individual converter controllers.

4 Conclusion

This paper has presented stability analysis, control design and tuning for power systems with VSC-based MTDC transmission systems. The assessments of the controls and components are supported by small signal stability analysis and verified by time domain simulation with EMT and RMS modes in DlgSILENT power factory. First, a point-to-point VSC-based HVDC is discussed and effects of different components of the network are analyzed. The system is found to be unstable for weak grid with $SCR < 1.75$ if power transfer by the converter is more than 0.5 pu. This instability is associated with integrator of the PLL of rectifier terminal. The investigated point-to-point VSC HVDC connection was expanded to a four terminal HVDC system. The critical poles associated with the dc link capacitor move towards imaginary axis which provokes the system to lose stability. Moreover, the negative real poles in point-to-point connection associated with current controller become oscillatory in MTDC system. The stability of MTDC system has been improved by ensuring optimized value of DC link capacitor and also by tuning the controller. Finally the full Cigré DC Grid test system has been studied, and details regarding the controllers and possible instability effects and oscillation modes in the system are discussed. The most oscillatory poles appear to be related to the DC link capacitor and other poles show similar behavior when it expands from point-to-point to MTDC.

Acknowledgement

The authors are very thankful to their organization for providing the opportunity for the research work.

References

- [1] N. Florentzou, V. G. Agelidis, G. D. Demetriades, "VSC-Based HVDC Power Transmission Systems: An Overview," in *IEEE Transactions on Power Electronics*, vol. 24, no. 3, March 2009, pp. 592-602
- [2] J. Glasdam, J. Hjerrild, L. H. Kocewiak, "Review on Multi-Level Voltage Source Converter Based HVDC Technologies for Grid Connection of Large Offshore Wind Farms," in *Proceedings of the 2012 IEEE POWERCON*, Auckland, New Zealand, 30 October – 2 November 2012, 6 pp.
- [3] S. Cole, T. K. Vrana, O. B. Fosso, J.-B. Curtis, A.-M. Denis, C.-C. Liu, "A European Supergrid: Present State and Future Challenges," in *Proceedings of the 17th PSCC 2011*, Stockholm, Sweden, 22-26 August 2011, 8 pp.
- [4] The North Seas Countries' Offshore Grid Initiative, information available from <https://www.entsoe.eu/about-entso-e/system-development/the-north-seas-countries-offshore-grid-initiative-nscog/> and <http://www.benelux.int/NSCOGI/>
- [5] Medgrid project, information available from: <http://www.medgrid-psm.com/en/project/>
- [6] Atlantic Wind Connection, information available from: <http://atlanticwindconnection.com/>
- [7] Beerten, J.; Cole, S.; Belmans, R., "Modeling of Multi-Terminal VSC HVDC Systems With Distributed DC Voltage Control," in *Power Systems, IEEE Transactions on*, vol.29, no.1, pp.34,42, Jan. 2014
- [8] O.A. Giddani, A. Y. M. Abbas, G. P. Adam, O. Anaya-Lara, K.L. Lo, "Multi-task control for VSC-HVDC power and frequency control," in *International Journal of Electrical Power and Energy Systems*, vol. 53, December 2013, Pages 684-690
- [9] C. Karawita and U. D. Annakkage, "Multi-Infed HVDC Interaction Studies Using Small-Signal Stability Assessment," in *IEEE Transactions on Power Delivery*, vol. 24, no. 2, April 2009, pp. 910–918, 2009
- [10] S. Cole, J. Beerten, R. Belmans, "Generalized Dynamic VSC MTDC Model for Power System Stability Studies," in *IEEE Transactions on Power Systems*, vol.25, no.3, August 2010, pp.1655-1662
- [11] N. R. Chaudhuri, R. Majumder, B. Chaudhuri, J. Pan, "Stability Analysis of VSC MTDC Grids Connected to Multimachine AC Systems," in *IEEE Transactions on Power Delivery*, vol.26, no.4, October 2011, pp. 2774-2784
- [12] G. O. Kalcon, G. P. Adam, O. Anaya-Lara, S. Lo, K. Uhlen, "Small-Signal Stability Analysis of Multi-Terminal VSC-Based DC Transmission Systems," in *IEEE Transactions on Power Systems*, Vol. 27, No. 4, November 2012, pp. 1818-1830
- [13] M. K. Zadeh, M. Amin, J. A. Suul, M. Molinas, O. B. Fosso, 'Small-Signal Stability Study of the Cigré DC Grid Test System with Analysis of Participation Factors and Parameter Sensitivity of Oscillatory Modes', accepted in PSCC 2014, August 18-22, 2014, Poland.
- [14] T. K. Vrana, Y. Yang, D. Jovcic, S. Dennezière, J. Jardini, H. Saad, "The CIGRE B4 DC Grid Test System", CIGRE Electra Magazine, 2013
- [15] T. Midtsund, J. A. Suul, T. Undeland, "Evaluation of Current Controller Performance and Stability for Voltage Source Converters Connected to a Weak Grid," in *Proceedings of the 2nd IEEE International Symposium on Power Electronics for Distributed Generation, PEDG 2010*, Hefei, China, 16-18 June 2010, pp. 382-388
- [16] J. Z. Zhou, A. M. Gole, "VSC transmission limitations imposed by ac system strength and ac impedance characteristics," in *Proceedings of the AC and DC Power Transmission Conference, ACDC 2012*, Birmingham, UK, 4-5 December 2012, 6 pp.